

Characterization of novel Ni–Al₂O₃–SiC nanocomposite coatings synthesized by co-electrodeposition

Mehran Masoudi · Mansor Hashim ·
Halimah Mohamed Kamari

Received: 18 December 2012 / Accepted: 13 June 2013 / Published online: 27 June 2013
© The Author(s) 2013. This article is published with open access at Springerlink.com

Abstract In the present work, Ni–Al₂O₃, Ni–SiC and novel Ni–Al₂O₃–SiC metal matrix composite (MMC) coatings were electrodeposited onto pure copper samples using a modified Watt's nickel electroplating bath containing nano alumina and silicon carbide particles with an average particle size of 50 nm. The composition, crystalline structure and surface morphology of the deposits were characterized by X-ray diffractometry (XRD), energy-dispersive X-ray spectroscopy (EDS) and field emission scanning electron microscopy (FESEM). The results indicated that Ni–Al₂O₃–SiC hybrid composite films with an acceptable homogeneity and granular structure having 9.2 and 7.7 % vol. Al₂O₃ and SiC nanoparticles, respectively were developed successfully. The nanoparticles incorporated in the nickel layer effectively increased the micro hardness and wear resistance owing to dispersion and grain-refinement strengthening, changing the nickel matrix morphology as well as the texture and preferred grain growth direction from <100> to the close-packed <111>. The oxidation resistance of the Ni–Al₂O₃–SiC hybrid composite coatings was measured to be approximately 41 % greater than the unreinforced Ni deposit and almost 30 % better than the Ni–Al₂O₃ composite coatings.

Keywords Nickel · Composite coating · Nanoparticles · Mechanical properties · Oxidation resistance

M. Masoudi (✉) · M. Hashim · H. M. Kamari
Department of Physics, Faculty of Science, Universiti Putra Malaysia (UPM), 43400 Serdang, Selangor, Malaysia
e-mail: mehranmasoudi@yahoo.com

M. Hashim
Advanced Materials and Nanotechnology Laboratory, Institute of Advanced Technology, Universiti Putra Malaysia (UPM), 43400 Serdang, Selangor, Malaysia

Introduction

Nanocomposite coatings consisting of dispersed pure metals, ceramics and organic ultrafine particles in a metallic matrix have attracted much attention from material scientists and engineers over the past few years due to their advanced physical, chemical and mechanical properties (Hovestad and Janssen 2005; Kim 2009; Zanella et al. 2009). A variety of coating techniques have been introduced for metal matrix composite coatings such as plasma spraying, physical vapor deposition (PVD) and electroplating of which the latter is a flexible, low-cost, low-temperature and quite a mature technique with well-studied controlling parameters and industrial applicability.

The Ni–SiC composites have been broadly investigated and successfully commercialized for the protection of parts subject to friction. This is due to the high level of hardness, excellent wear resistance and low production cost of the SiC particles. The Ni–SiC composite coatings exhibit a combination of significant hardness, good ductility and low internal stress. These metal matrix composite (MMC) coatings have an improved high-temperature oxidation resistance compared to pure Ni films, since the formation of SiO₂ at elevated temperatures reduces the rate of the outward diffusion of Ni atoms to the oxidation front and retards NiO formation (Garcia et al. 2001; Lee and Lee 2008; Lin and Huang 2004; Pavlatou et al. 2006; Zhou and Ding 2007).

The Ni–Al₂O₃ composite coating is used primarily to increase the surface microhardness and wear resistance of metallic parts. Implanting alumina fine particles in a nickel matrix improves the mechanical properties and the thermal stability of the nickel coatings. The Ni–Al₂O₃ composite films almost triple the yield stress value and up to twice the wear resistance of pure nickel. The thermal stability of the

Ni–Al₂O₃ MMC films is noticeably better than the pure nickel layer, since the dispersed alumina ceramic particles suppress sliding dislocations, grain boundary movements and the re-crystallization process at elevated temperatures (Jung et al. 2009; Góral et al. 2010; Feng et al. 2008; Gheorghies et al. 2006; Gül et al. 2009; Wang et al. 2003).

In the present study, novel Ni–Al₂O₃–SiC nanocomposite coatings were prepared by a co-electrodeposition technique to achieve a combination of improved tribological properties, high-temperature oxidation resistance and thermal stability. The crystalline structure, surface morphology, microhardness, wear and high-temperature oxidation resistance of these newly introduced hybrid composite films were investigated and compared with the pure nickel film and Ni–Al₂O₃ as well as Ni–SiC nanocomposite coatings.

Experimental aspects

Co-electrodeposition

The pure Ni, Ni–Al₂O₃, Ni–SiC and Ni–Al₂O₃–SiC nanocomposite coatings were prepared using an electroplating technique employing a typical Watt's bath. The bath composition and plating conditions were as listed in Table 1. De-ionized water was used to prepare the plating electrolyte. An amount of 50 g/l nano α -alumina and silicon carbide particles of 99.5 % purity with an average diameter of 50 nm (Qinhuangdao TaijiRing Nano-Products Company) were added to fresh nickel electrolyte in each case. The powders were used as received from the manufacturer without any further treatment. Prior to the co-deposition, the nanoparticles were dispersed in the bath by using a magnetic stirrer at 600 rpm for 4 h and then ultrasonically mixed for 45 min. The temperature of the electrolyte was maintained at 45 ± 1 °C by an automatic temperature controller. The solution pH was monitored and

maintained at 4.0 ± 0.2 using 0.1 mol HCl and 0.05 mol NaOH solutions. Each experiment was carried out using a fresh solution.

A pure copper plate of 30 mm \times 10 mm \times 1 mm size was used as the cathode; the anode was a pure Ni plate (99.98 %) with an area of 10 cm². Before co-deposition, the copper samples were mechanically polished to a 2,000-grit finish, cleaned in a 0.1 mol NaOH solution and finally activated in 5 % hydrochloric acid at room temperature. The electrolyte bath was mechanically stirred constantly at 250 rpm during the electroplating course. After the co-deposition process, the samples were washed with distilled water and cleaned by ultrasound for 15 min to remove any loose particles from the surface.

Coating characterization

The microstructure and surface morphology of the electroplated coatings were studied by X-ray diffraction (Cu–K α) at room temperature with a scan rate of $0.15^\circ \text{min}^{-1}$ over a 2θ range of $10\text{--}90^\circ$ and also field emission scanning electron microscopy (FESEM, Nova Nano SEM–2300). The amount of incorporated particles in the nickel matrix was evaluated using an energy-dispersive X-ray spectroscopy (EDS) analyzer connected to the FESEM and micrograph image processing. The mean diameter of the nanoparticles and the deposit film grain size were determined by using the Scherrer method, disregarding microstrains. The texture of the electrodeposits was determined by the texture coefficient, *TC*, defined as follows:

$$TC = \left(\frac{I}{I_0} \right) / \left(\frac{1}{n} \cdot \sum \frac{I}{I_0} \right) \quad (1)$$

where *I* and *I*₀ are the X-ray diffraction intensities of the (*hkl*) plane in an experimental specimen and a standard powder sample (given in the JCPDS data), respectively; *n* is the number of planes.

The hardness of the pure nickel and nanocomposite coatings was determined using a Vickers microhardness measuring device. The test was performed under a 100 g load and the corresponding final values were determined as the average of a minimum of five measurements. The wear tests were performed at room temperature by measuring the weight lost during grinding of the samples on a 2,000-grit SiC waterproof paper. The mass losses of the samples, to an accuracy of 0.1 mg, were recorded to determine the wear resistance of the deposits. The wear tests were repeated three times on each sample and with different sliding distances to minimize the error and data scattering. The Archard equation (Eq. 2) was used to analyze the wear test results and determine the wear coefficient of the pure nickel, Ni–Al₂O₃, Ni–SiC and Ni–Al₂O₃–SiC films.

Table 1 Electrolyte composition and plating parameters

Component	Concentration (g/l)
NiSO ₄ ·6H ₂ O	240
NiCl ₂ ·6H ₂ O	40
H ₃ BO ₃	35
CH ₃ (CH ₂) ₁₁ OSO ₃ Na	0.2
Deposition condition	Value
pH	4
Time (min)	45
Temperature (°C)	45
Current density (A/dm ²)	5

$$W = K \cdot F \cdot S \quad (2)$$

$$K = K_0 / H \quad (3)$$

where W is the wear volume lost, K_0 is the wear coefficient, K is the dimensional wear coefficient, H is the hardness, F is the normal force, and S is the sliding distance.

Thermal oxidation was investigated using an electric muffle furnace. The experiments were carried out at 1,173 K for different exposure times. After the high-temperature oxidation tests, the samples were cooled in air and weighed using an electronic balance with a ± 0.01 mg accuracy to determine the weight gain in mg/cm^2 . As oxidation is a diffusional thermally activated process, the oxidation rate constant can be calculated by considering the Eq. 4 as follows:

$$\left(\frac{\Delta w}{A}\right)^2 = K_{ox} \cdot t \quad (4)$$

where $(\Delta w/A)$ is the weight changes per unit area, K_{ox} is the oxidation rate constant and t stands for the oxidation time.

Results and discussion

Characterization of the nanoparticles

Figure 1a, b shows the XRD patterns of the SiC and Al_2O_3 nanoparticles which match with hexagonal silicon carbide and trigonal alumina reference peaks. The average particle sizes of the Al_2O_3 and SiC powders were calculated to be 79 and 37 nm, respectively, by using the three main peaks of the X-Ray diffraction in the Scherrer equation disregarding the effect of microstrains. The SEM observations also showed that the as-received SiC and Al_2O_3 powders had spherical and coarse shapes, respectively, with diameters between 41 and 85 nm (Fig. 2). Thereafter, the nominal size of 50 nm as given by the manufacturer was accepted as the average value.

By using the characteristic peak broadening of the co-deposited silicon carbide and alumina particles in the hybrid composite layer (Fig. 1f), the embedded Al_2O_3 and SiC mean particle sizes were estimated at approximately 64 and 73 nm, respectively. These results and also the SEM micrographs (Fig. 3) show no noticeable particle agglomeration in the formed composites.

Coating particle content

The amount of implanted particles in composite films is affected by a number of variables such as electrolyte composition and electroplating controlling parameters, the physical and chemical properties of the particles, hydraulic forces during the mixing and probable interaction between

the particles. The surface energy and molecular polarization of the suspended particle initiate a type of physical adsorption of the ions on the surface of the neutral particles. The ion cloud around the particles creates a driving force to move the particles toward the cathode surface. If the concentration polarization near to the cathode is considered to be negligible, combinations of electrical and hydraulic forces define the probability of particle adsorption.

The volume percentages of embedded alumina and silicon carbide particles in the Ni–SiC, Ni– Al_2O_3 and Ni– Al_2O_3 –SiC composite coatings were determined by an EDS analyzer and the image processing using dark field micrographs (Fig. 4) as shown in Table 2. The Al_2O_3 deposition rate was higher than that of the SiC in the mono and hybrid composites, which could be attributed to the high surface energy and polarity of the alumina. The particle content of the Ni– Al_2O_3 –SiC was less than the total co-deposited particles in the Ni– Al_2O_3 and Ni–SiC layers due to probable interaction between the particles in the electrolyte and over the cathode surface.

Microstructure and morphology

The average grain size of the deposited films was calculated using the Scherrer equation by considering the (220) plane peak broadening with the values in the nanometer range as shown in Table 2. As a general result, the nickel matrix grain size was reduced in the presence of the dispersed particles. This grain refinement can be explained by considering the influence of the implanted particles in terms of increasing the nickel nucleation rate and suppressing crystal grain growth. The Ni, Ni–SiC and Ni– Al_2O_3 exhibited preferred grain growth in the $\langle 110 \rangle$, $\langle 100 \rangle$ and $\langle 111 \rangle$ crystalline directions, respectively, and the hybrid Ni– Al_2O_3 –SiC grain growth orientation was determined to be in the close-packed $\langle 111 \rangle$ direction similar to that for Ni– Al_2O_3 nanocomposite coatings. The calculated texture coefficients (Table 3), illustrate that the formed Ni– Al_2O_3 and hybrid Ni– Al_2O_3 –SiC composite films almost do not have a texture and instead show a homogeneous grain growth in random crystalline directions in contrast to the pure nickel and Ni–SiC which showed a texture in the $\langle 110 \rangle$ direction.

The pure nickel film SEM micrograph in Fig. 3a indicates a rough surface columnar structure. The cross section and surface micrographs of the Ni– Al_2O_3 composite coatings shown in Fig. 3b, c portray a regular granular grain structure with an almost homogeneous distribution of alumina particles in the composite layer of average thickness of 36 μm . Figure 3d–f) shows the morphology and distribution of the SiC particles in the Ni–SiC composite layer. These micrographs exhibit a columnar structure which is a characteristic of nickel coatings plated in a nickel Watt's

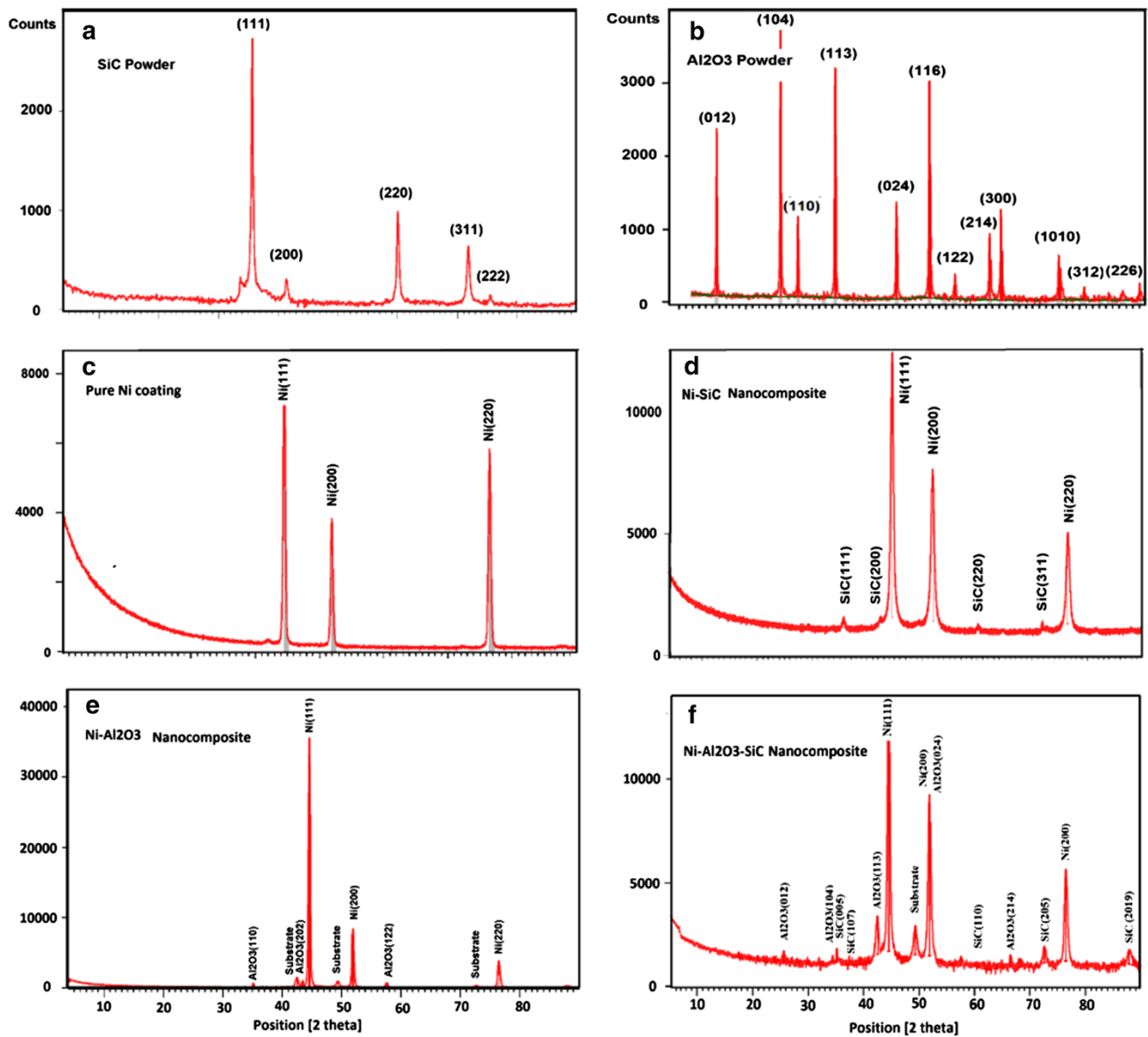
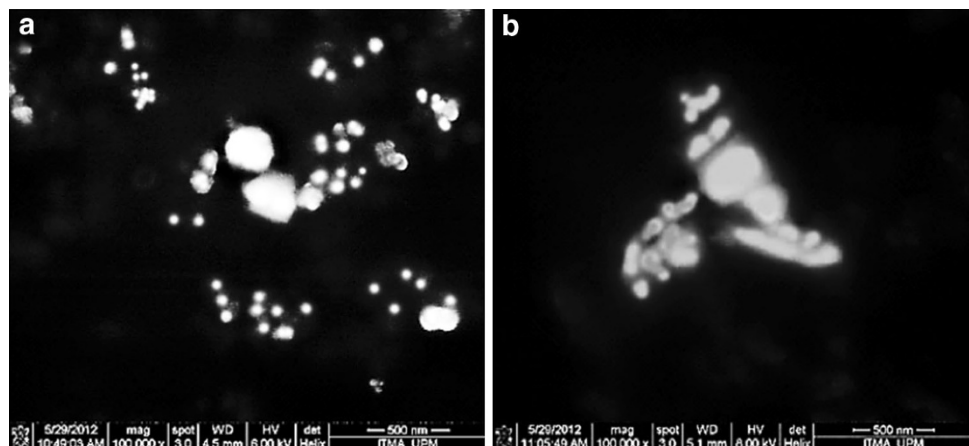


Fig. 1 XRD pattern of: **a** silicon carbide powder, **b** alumina powder, **c** pure nickel coating, **d** Ni–SiC composite, **e** Ni–Al₂O₃ composite, **f** Ni–Al₂O₃–SiC hybrid composite

Fig. 2 Nano powders FESEM micrographs. **a** SiC (100,000X), **b** Al₂O₃ (100,000X)



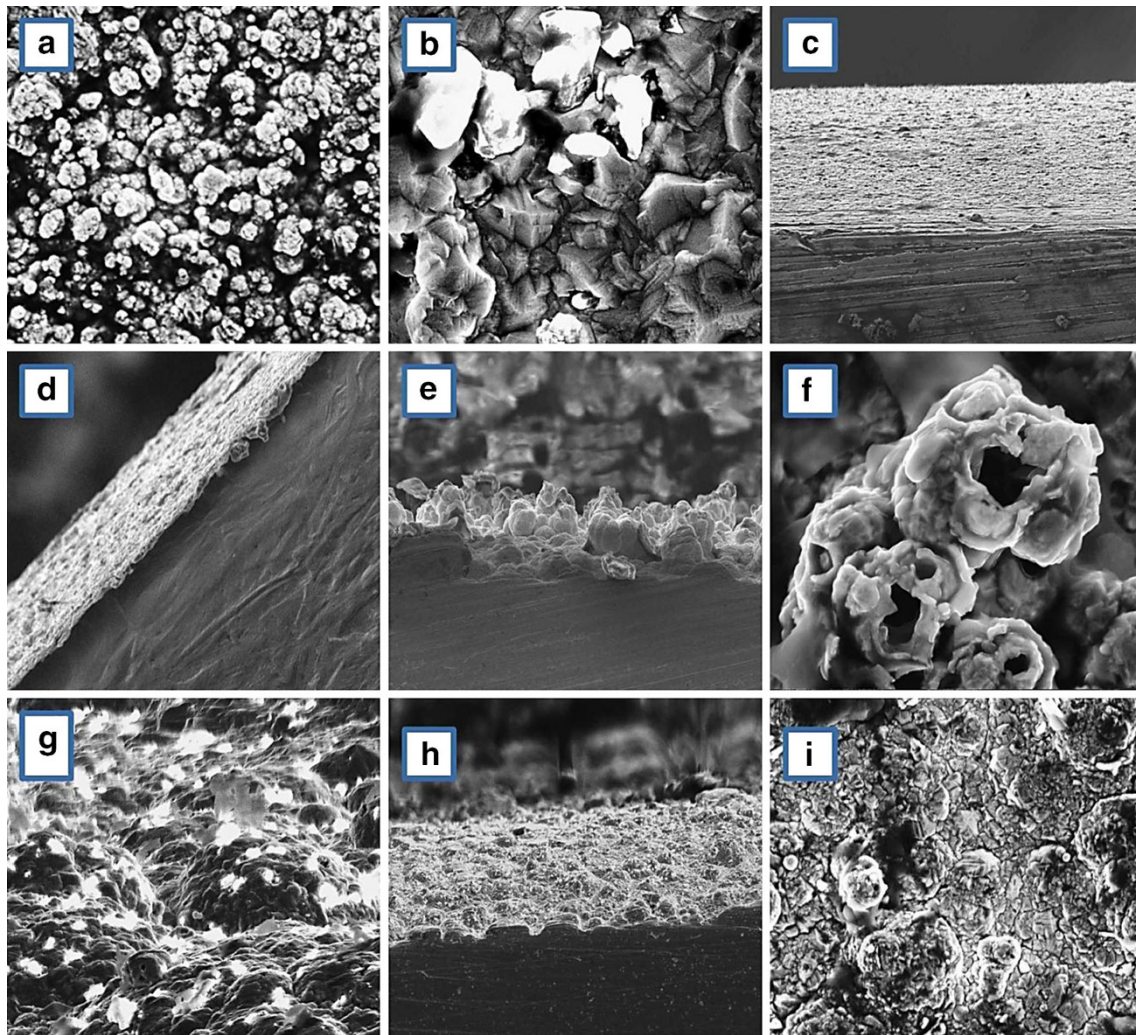


Fig. 3 **a** Pure Ni (10,000X), **b** Ni–Al₂O₃ surface micrograph (4,000X), **c** Ni–Al₂O₃ coating cross section (3,000X), **d** Ni–SiC cross section (2,000X), **e** Ni–SiC cross section (1,000X), **f** Ni–SiC

columnar structure (40,000X), **g** Ni–Al₂O₃–SiC (30,000X), **h** Ni–Al₂O₃–SiC cross section(2,000X), **i** Ni–Al₂O₃–SiC surface granular structure(10,000X)

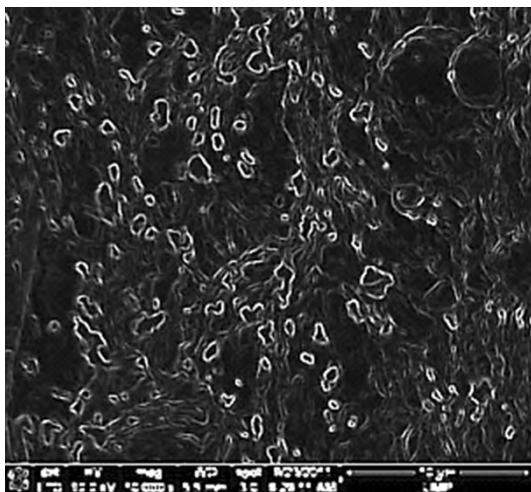


Fig. 4 Dark field micrograph of the hybrid Ni–Al₂O₃–SiC nano-composite coating (10,000X)

Table 2 Test results

Coating	Particle content %Vol.	Grain size (nm)	Hardness (HV)	Wear Coefficient × E-16
Ni	–	103	295	3.1
Ni–SiC	9.3	41	456	1.5
Ni–Al ₂ O ₃	13.1	18	588	1.3
Ni–Al ₂ O ₃ –SiC	9.2, 7.7	25	767	0.9

bath. The Ni–SiC films show a high density of surface porosity. The hybrid Ni–Al₂O₃–SiC composite coating SEM micrographs (Fig. 3g, i) show a compact granular structure. The cross section of the hybrid composites (Fig. 3h) confirmed the homogeneous distribution of fine particles in the composite layer.

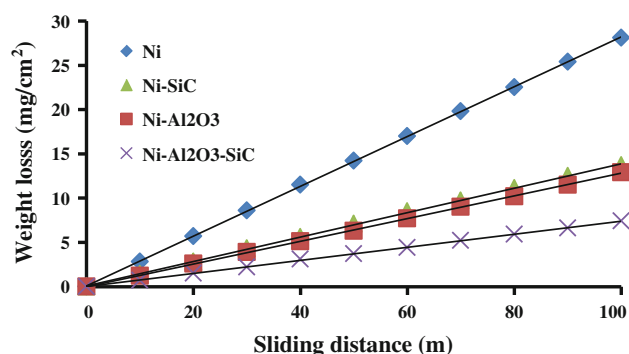
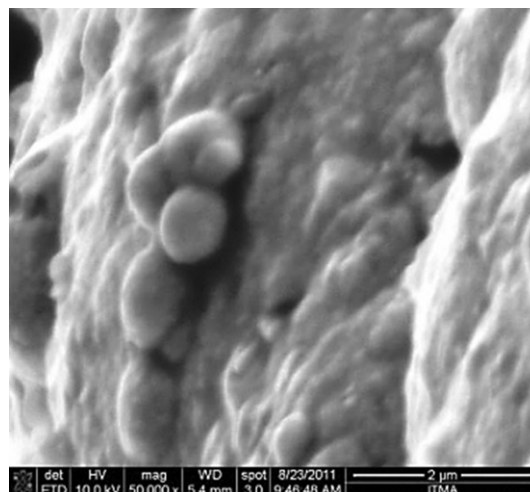
Table 3 Texture coefficient of deposit layers

Texture coefficient (TC)				
Crystalline direction	Ni	Ni–SiC	Ni–Al ₂ O ₃	Ni–Al ₂ O ₃ –SiC
111	8.9	32.2	32.3	35.4
100	10.1	27.8	26.3	39.6
110	81	50.3	30.7	31.2

Microhardness and wear resistance

The microhardness test results of the pure nickel and nickel composite coatings are shown in Table 2. The results show that adding dispersed particles to the nickel layer significantly enhances the microhardness. This improvement is mainly related to the Hall–Petch hardening effect (grain-refinement strengthening) and incorporation of nanoparticles (dispersion strengthening), which inhibits the plastic flow of the metal matrix by blocking the free sliding of the dislocations. Furthermore, a portion of the enhanced hardness can be correlated to the influence of the particles on the morphology and crystalline structure of the coatings. Ni–Al₂O₃–SiC shows superior hardness of 2.6 times higher than pure Ni and 30 % above Ni–Al₂O₃ coatings due to the synergetic effects of grain refining and dispersive strengthening, whereas Ni–Al₂O₃–SiC has a higher particle content, finer granular grain structure and a grain growth in the close-packed hard $\langle 111 \rangle$ direction.

The graph of weight lost after the sliding test for the nickel and nickel nanocomposite coatings is shown in Fig. 5. The Ni–Al₂O₃–SiC hybrid composite coating showed the maximum wear resistance followed by the Ni–Al₂O₃ and Ni–SiC deposits. The wear resistance of the newly introduced hybrid composite coatings was more than three times higher than the nickel films and approximately 75 % better than those of monocomposites of Ni–SiC and Ni–Al₂O₃. The calculated dimensional wear coefficient factors for the tested samples using Eqs. (1) and (2) for 100 m sliding distance are shown in Table 2, which

**Fig. 5** Wear test results**Fig. 6** Spherical particles on the surface of the Ni–Al₂O₃–SiC MMC film (50,000X)

confirms the superior wear resistance of the Ni–Al₂O₃–SiC nanocomposite. It is suggested that combining the nickel-base ductility and the excellent wear resistance and toughness of the silicon carbide and alumina produced a good load-bearing capacity and delaminating resistance. The projected hard particles on the coating surface increase the sliding wear resistance. Moreover, sphere-shaped SiC nanoparticles released from the composite surface (Fig. 6) may change the sliding friction into a rolling mode and reduce the wear rate.

High-temperature oxidation test

Figure 7 shows the XRD patterns of the Ni–Al₂O₃–SiC hybrid composite coating oxidized at 1123 K for 25 h, which indicates that the oxide scale formed is composed of NiO, Al₂O₃, Ni₂SiO₄ and SiO₂. Spinel nickel aluminate oxide (NiAl₂O₄) after the 25 h oxidizing test was not detected. This could be due to an inadequate alumina concentration and a low diffusion rate of nickel atoms inside the alumina particles. SEM studies (Figure 8) and the XRD analysis of the Ni–Al₂O₃–SiC hybrid composite coating show that a condensed oxide scale formed during the oxidation test. The exposed nickel on the surface was oxidized at the beginning of the oxidation test at elevated temperatures, and as the oxidation proceeded, SiO₂ oxide formed and reacted with NiO to form Ni₂SiO₄ which decreased the diffusion rate of the nickel and oxygen in opposite directions.

The high-temperature oxidation test results in the graphs in Fig. 9 illustrated that the formed Ni–Al₂O₃–SiC had a 30 % higher oxidation resistance compared to the Ni–Al₂O₃ nanocomposite coatings and was about 41 % better than the nickel deposits. The curves in Fig. 10 show almost

Fig. 7 XRD test result of Ni–Al₂O₃–SiC MMC film after tempering at 1,123 K for 25 h

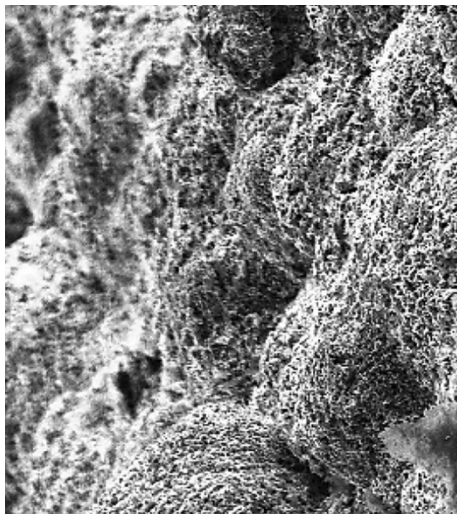
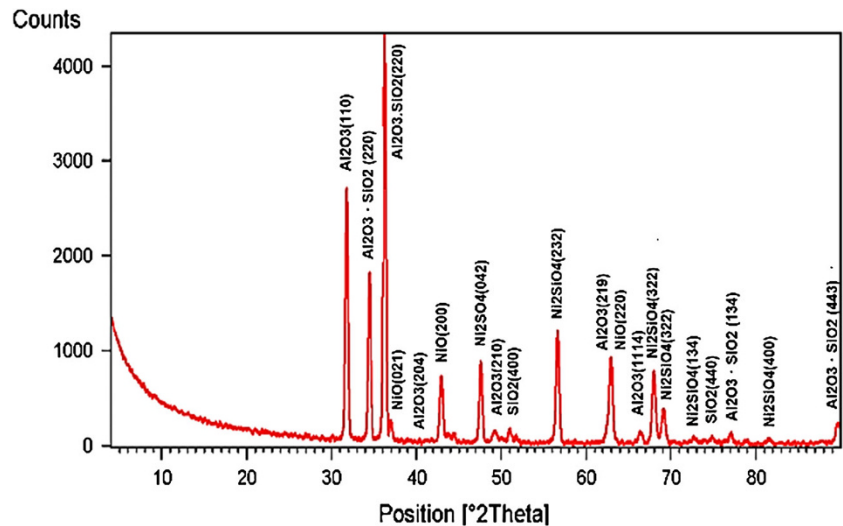


Fig. 8 SEM micrograph of the Ni–Al₂O₃–SiC film tempered at 1,123 K for 25 h (3,000X)

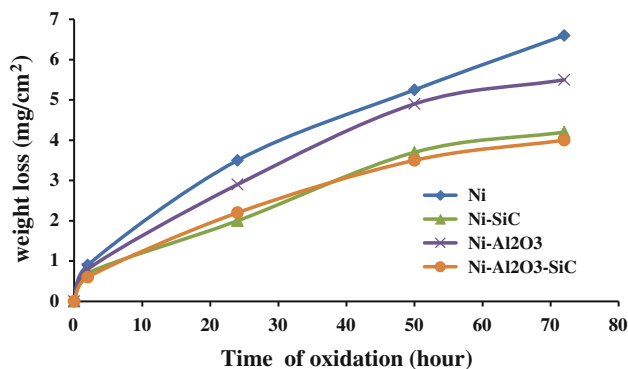


Fig. 9 High-temperature oxidation test result of Ni–Al₂O₃–SiC MMC film at 1,123 K

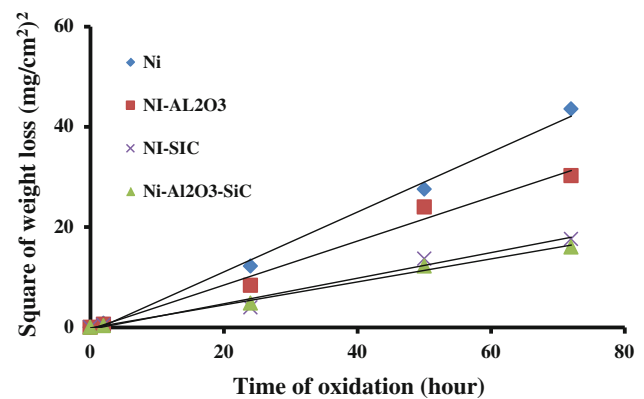


Fig. 10 The square of weight changes against time for the high-temperature oxidation test result of Ni–Al₂O₃–SiC MMC film at 1,123 K

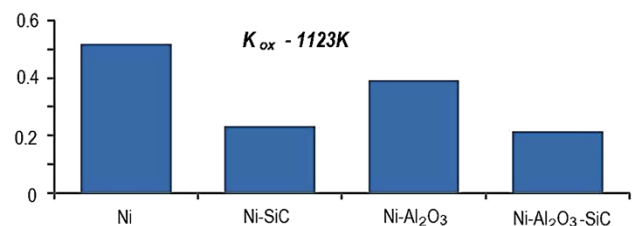


Fig. 11 Dimensional wear coefficient factor of coated samples and pure nickel film

a linear relationship between the square of the weight changes against time of the oxidation test for all mono and hybrid composite coatings and show a good agreement with the diffusion model of oxidation with a moving interface as explained by Eq. 4. Figure 11 shows the oxidation rate constant (K_{ox}) for the tested deposits, which match the oxidation test results and confirm the improved

high-temperature oxidation resistance of the hybrid Ni–Al₂O₃–SiC composite in comparison with the MMC Ni–Al₂O₃ and pure Ni films.

Conclusion

Ni matrix hybrid MMC coatings reinforced with a homogeneous dispersion of nano Al₂O₃ and SiC particles were successfully produced by co-electroplating using a modified Watt's type electrolyte. Implanting SiC in a well-commercialized Ni–Al₂O₃ MMC coating formed new Ni–Al₂O₃–SiC nanocomposite films with improved high-temperature oxidation resistance without reduction in the advanced tribological and mechanical properties of the Ni–Al₂O₃ MMC coatings. The implanted nano size particles decreased the nickel matrix grain sizes from above 100 to 25 nm and this led to a type of grain refinement and loss of texture. The morphology as well as the microstructure of the nickel matrix significantly altered in the presence of the dispersed nanoparticles. The Ni matrix preferred grain growth orientation changed from <110> to the <111> direction in the Ni–Al₂O₃–SiC MMC films. The SEM micrographs showed that the pure nickel and the Ni–SiC composite had a rough surface columnar morphology, whereas the Ni–Al₂O₃ and Ni–Al₂O₃–SiC composite coatings portrayed a compact granular structure. The introduced hybrid MMC films showed 2.6 times higher microhardness compared to the Ni films and 30 % better than the Ni–Al₂O₃ nanocomposite coatings. The wear resistance of the Ni–Al₂O₃–SiC MMC films was measured to be almost four times higher than pure nickel and 75 % better than the Ni–SiC/Al₂O₃ composite coatings. The high-temperature oxidation test results at 1173 K indicated that the Ni–Al₂O₃–SiC coatings had an enhanced oxidation resistance of 30 % higher than the Ni–Al₂O₃ nanocomposite coating and 41 % better than the nickel deposit due to forming a compact oxide scale which consisted of SiO₂, Al₂O₃, NiO and NiSi₂O₄ on the hybrid composite surface. These properties make the Ni–Al₂O₃–SiC hybrid composite a good candidate coating for protection of specimens subject to severe mechanical working conditions and elevated temperatures.

Acknowledgments This research was supported by the Advanced Materials and Nanotechnology Laboratory, Institute of Advanced

Technology, Universiti Putra Malaysia, 43400 UPM Serdang, Selangor, Malaysia.

Open Access This article is distributed under the terms of the Creative Commons Attribution License which permits any use, distribution, and reproduction in any medium, provided the original author(s) and the source are credited.

References

- Feng Q, Li T et al (2008) Investigation on the corrosion and oxidation resistance of Ni–Al₂O₃ nano-composite coatings prepared by sediment co-deposition. *Surf Coat Technol* 202(17):4137–4144
- Garcia I, Fransaer J, Celis J (2001) Electrodeposition and sliding wear resistance of nickel composite coatings containing micron and submicron SiC particles. *Surf Coat Technol* 148(2–3):171–178
- Gheorghies C, Carac G, Stasi IV (2006) Preparation and structural characterization of nickel/alumina nano-particles composite coatings. *J Optoelectron Adv Mater* 8(3):1234–1237
- Góral A, Beltowska-Lehman E, Indyka P (2010) Structure characterization of Ni/Al₂O₃ composite coatings prepared by electrodeposition. *Solid State Phenom* 163:64–67
- Gül H, Killıç F, Aslan S, Alp A, Akbulut H (2009) Characteristics of electro-co-deposited Ni–Al₂O₃ nano-particle reinforced metal matrix composite (MMC) coatings. *Wear* 267(5–8):976–990
- Hovestad A, Janssen L (2005) Electroplating of metal matrix composites by co-deposition of suspended particles. *Modern aspects of electrochemistry*, Springer USA, 38:475–532
- Jung A, Natter H, Hempelmann R (2009) Nanocrystalline alumina dispersed in nanocrystalline nickel: enhanced mechanical properties. *J Mater Sci* 44:2725–2735
- Kim MJ (2009) Oxide-dispersed nickel composites and the behavior of their mechanical properties. *Met Mater* 15(5):789–795
- Lee Hong-Kee, Lee Ho-Young (2008) Electrolytic deposition behaviours of Ni–SiC composite coatings containing submicron-sized SiC particles. *Met Mater Int* 14(5):599–605
- Lin CS, Huang KC (2004) Co-deposition and microstructure of nickel–SiC composite coating electrodeposited from sulphamate bath. *J Appl Electrochem* 34(10):1013–1019
- Pavlatou EA, Stroumbouli M, Gyftou P, Spyrellis N (2006) Hardening effect induced by incorporation of SiC particles in nickel electrodeposits. *J Appl Electrochem* 36(4):385–394. <http://link.springer.com/article/10.1007/s10800-005-9082-y>
- Wang TC, Chen Z, Tuan WH (2003) Oxidation resistance of Ni-toughened Al₂O₃. *J Eur Ceram Soc* 23(6):927–934. <http://ntur.lib.ntu.edu.tw/bitstream/246246/95443/1/38.pdf>
- Zanella C, Lekka M, Bonora PL (2009) Influence of the particle size on the mechanical and electrochemical behaviour of micro- and nano-nickel matrix composite coatings. *J Appl Electrochem* 39:31–38. doi:10.1007/s10800-008-9635-y
- Zhou Y-B, Ding Y-Z (2007) Oxidation resistance of co-deposited Ni–SiC nanocomposite coating. *Trans Nonferr Met Soc China* 17(5):925–928